Available online at www.sciencedirect.com
ScienceDirect
Journal of Photochemistry and Photobiology A: Chemistry 196 (2008) 165–173
Journal of Photochemistry and Photobiology A:Chemistry
www.elsevier.com/locate/jphotochem

Tailoring the activity of Ti-based photocatalysts by playing with surface morphology and silver doping

M.J. Uddin, F. Cesano, S. Bertarione, F. Bonino, S. Bordiga, D. Scarano, A. Zecchina *

Nanostructured Interfaces and Surfaces (NIS), Centre of Excellence, Department of Chemistry IFM, University of Turin, Via P. Giuria 7, I-10125 Torino, Italy

Available online 23 August 2007

Abstract

TiO_2 thin films have been prepared on cotton fibres by using sol–gel method at low temperature (∼100 °C) and metallic Ag nanoparticles were deposited on porous TiO_2 film by photoreduction. The Ag–TiO_2 covered cotton fibres show multichromic behaviour under visible and UV light exposure as well as photoactivity [M.J. Uddin, F. Cesano, F. Bonino, S. Bordiga, G. Spoto, D. Scarano, A. Zecchina, J. Photochem. Photobiol. A: Chem., 89 (2007) 286-294]. The developed multiactive cotton fibres show grey colour under visible light and change their colour reversibly to deep brown upon ultraviolet light exposure. The original and treated fibres have been characterized by several techniques (SEM, AFM, EDS microanalysis, Raman, UV–vis spectroscopy, XRD and TGA) and the Ag–TiO_2 nanoparticles have been found to form an homogeneous thin film on the fibre surface.

Keywords: Photochromism; Photocatalysis; Thin film; Silver-doped TiO_2; Ag/TiO_2–cotton composite fibres

1. Introduction

Nanosized anatase TiO_2 is known to have a wide range of applications in photocatalysis, gas sensing, etc. [1]. Due to the large surface area [2], thin film coatings consisting of anatase TiO_2 nanoparticles show high photocatalytic efficiency. The optical properties and the photocatalytic activity of TiO_2 coatings do not depend only on the phase, but also on the crystallite size and porosity [3]. Development of TiO_2-based photocatalysts anchored to large surface area supporting materials (usually inorganic), where pollutants are efficiently condensed, are of great significance, because of the high photodecomposition efficiency [4] and of advantages associated with filtration of the suspension of fine photocatalyst particles. Sol–gel derived titanium dioxide composites have been also developed and investigated for the purpose of producing thin films and self-supported photocatalysts. The resulting photocatalysts exhibit relatively high surface area and enhanced mechanical stability and integrity [5]. TiO_2 films have been deposited also on organic support-like cellulose fibres [6]. These films show a high photodecomposition efficiency and the supporting material is stable under prolonged illumination. It is well known that the initiation step of the photocatalytic process consists in the generation of electron–hole pairs upon irradiation of the material with a photon having energy at least equal to that of the band gap of the photocatalyst. The electron–hole pairs formed can either recombine in the bulk or travel up to the surface, where they can participate in chemical reaction involving species adsorbed on the external titanol groups. The only drawback of TiO_2 is that its band gap lies in the near-UV of the electromagnetic spectrum: 3.2 eV (285 nm) and 3.0 eV (410 nm) for anatase and rutile, respectively. As a consequence, only UV light is able to create electron–hole pairs and to initiate the photocatalytic processes. It is therefore evident that any modification of the TiO_2-based photocatalysts, resulting in a lowering of its band gap [7] or in the introduction of stable optical sensitizers [8], is representing a breakthrough in the field. This is the reason why so many scientific works have appeared during recent years. An exhaustive analysis of the different approaches used to dope TiO_2 is beyond of scope of this contribution and only a selection of cases will be summarized below. (i) One case is doping TiO_2 with various transitions metals such as Au, Ag, Pt, Cr, Nb, V, Mn and Fe [9–14]. These systems show an enhanced photoactivity in the visible with an efficiency depending highly on the preparation method. However, they are characterized by thermal instability and by a critical control of the cluster dimension and distribution [11]. (ii) Another case is represented by

* Corresponding author. Tel.: +39 011 6707860; fax: +39 011 6707855.
E-mail address: adriano.zecchina@unito.it (A. Zecchina).

1010-6030/$ – see front matter © 2007 Elsevier B.V. All rights reserved.
doi:10.1016/j.jphotochem.2007.07.037

TiO_2 doped with nonmetals atoms such as N [15–20], S [21,22], F [23], C [7,17,24,25], I [26,27], Br [28] and Cl [28]. In particular, as far as iodine doping is worked, it has been demonstrated that also molecular I_2 trapped inside internal nanovoids of TiO_2 is able to promote photoactivity [27]. Also in this case the photocatalytic activity depends on the content of nonmetal atoms and on the method of preparation. (iii) A third case is a dye sensitized TiO_2 obtained by anchoring a dye on the surface of the photocatalyst [8]. Various dyes (catechol [29], porphyrins [30], phthalocyanines [31], etc.) have been employed as sensitizers, but most of them are toxic and, more important, easily undergo a self-degradation process, that makes them unsuitable for durable applications in photocatalysis. The photocatalytic activity of microporous titanosilicates ETS-10 and ETS-4 has also been recently investigated [32–38]. Due to the large internal surface area, these microporous photoactive materials are potentially very interesting. Unfortunately, the fact that Ti atoms are organized in one-dimensional linear chains of TiO_6 octahedra (–O–Ti–OTi–), behaving as semiconducting nanowires [39–43], causes a blue shift of the band gap with the consequence that photocatalytic activity in the visible region is suppressed. To overcome this drawback, Klabunde and co-workers [44] have introduced transition metal ions in ETS-10 either by addition of the corresponding salts during the synthesis (Cr and Co samples with Cr (or) Co/Ti = 0.05) or by a postsynthesis ion-exchanged approach (Co and Ag). (iv) As a fourth case TiO_2 doped with silver particles must be mentioned. The so obtained systems show antimicrobial activity [45–53]. For this reason TiO_2-Ag coatings are used for catheters [45,46] and have also been incorporated into bioglass [47]. Brook et al. [54] have described that Ag–TiO_2 films are not only active as disinfectants but also exhibit "self-regeneration" capability, because they both kill bacteria present on the film surface and photodegrade the residues. Such a dual action is significantly reducing the problems of surface deactivation due to build up of contamination. Recently it has been shown that Ag-TiO_2 films on Pyrex glass show also multicolour photochromism [55] and photoinduced conversion of Ag nanoparticles [56] due to surface plasmon resonance effects. The multicolour behaviour of Ag particles on TiO_2 depends upon the particle size, shape and local refractive index [50,56]. The explanation of this effect is that under UV light, electrons in the valence band of TiO_2 are excited to the conduction band, with formation of holes in the valence band. At the same time electrons of Ag nanoparticles, when irradiated with the light of their plasmon resonance wavelength, are excited and transformed to adsorbed oxygen with formation of O_2^-. The Ag nanoparticles are consequently oxidized by O_2^- to colourless Ag^+ ions [57]. In presence of TiO_2 these Ag^+ ions are reduced by the excited electrons and Ag nanoparticles are reformed [58].

In our previous work [6], we described a simple and repeatable anchoring procedure of a TiO_2 nanophase on the cellulose fibres. The so obtained TiO_2 films show high photostability upon prolonged exposure to light and photoactivity in multiple pollutant adsorption–photodegradation cycles. The interest of these coatings relies on the fact that they can find application in self-cleaning of fabrics. In addition, the stability to washing test [6] suggests that the anchoring process of the particles involves the formation of chemical bonds, for example via esterification of the surface OH groups with titanols. Another interesting point under investigation is related to the fact that TiO_2 support can be eliminated by burning in oxygen, leaving behind TiO_2 structures in forms of tubings (unpublished results).

For the reasons briefly mentioned above, we became interested in modifying the light absorbing property and antibacterial activity of Ag-TiO_2 films covering the cotton fabrics. Coming now to this study, it can be divided into three parts. In the first part we illustrate a new strategy to synthesize a silver-doped titanium dioxide characterized by the presence of large surface area. In the second part, we demonstrate that the layer consists of anatase, which is efficient to remove the adsorbed molecular species from the environment via photocatalytic reaction [6]. In the third part, on the basis of the experience acquired on the deposition of TiO_2 films on the cellulose fibres, we evaluate the possibility to develop photochromic properties on cotton fibres, covered by silver-doped TiO_2. A study concerning the evaluation of antibacterial properties is in progress.

To evaluate the crystalline phases and to control possible changes on the crystallinity and on the morphology before and after the silver-doping treatments, X-ray powder diffraction (XRD), scanning electron microscopy (SEM) and atomic force microscopy (AFM) have been applied. Raman spectroscopy has been used to confirm the presence of anatase TiO_2 and to follow the stability of the film. UV–vis–NIR allows us to evaluate the optical properties of the synthesized Ag–TiO_2 film present on the natural fibre support. Finally to test the photochromic activity of the Ag–TiO_2 on the fibre support, the optical properties analyzed with UV–vis spectroscopy in reflectance mode have been investigated. To the best of our knowledge, the results illustrated in this contribution show that we have developed new photochromic thin films deposited on cotton textiles at low temperature, with potential challenging applications.

2. Experimental

2.1. Materials

Pure cotton fibres, 10–15 μm in diameter, from PVS srl (Milano, Italy) were used for the entire process. All chemicals used in this work were procured from Aldrich, Germany, and have been used as received. Water used in our experiments was triple distilled and produced in our laboratory.

2.2. Synthesis of Ag–TiO_2 thin film

The procedure for the formation of Ag–TiO_2-coated cotton fibres consists of 4 stages. In stage 1, the impurities (fat, wax, etc.) of the fibres have been removed by soxhlet extraction with acetone for 30 min. Then the fibres have been dried at room temperature for 12 h. In stage 2, a solution of Titanium isopropoxide (TIP) was mixed with a second aqueous solution prepared separately containing dilute HCl and $(CH_3)_2CHOH$, following the procedure described in reference [6] and mixed together by magnetic stirring (200 rpm). The resulting sol was

transparent and quite stable and can be used to impregnate cotton fibres. In stage 3, the extracted samples were placed in a preheated oven at 70 °C, in order to remove the solvent from the fibres, then cured at 95 °C for 5 min to complete the formation of TiO_2 from the precursor. Finally, the impregnated cotton fibre samples were treated in boiling water for 3 h (post-curing). This step also removes the unattached TiO_2 particles from the fibre surface. In stage 4, the resultant samples dried in a preheated oven at 50 °C, were soaked in 0.001 M $AgNO_3$ aqueous solution for 1 min. The sample was then dried at room temperature. For photochromic studies, the sample with $AgNO_3$-TiO_2 thin film was irradiated at 308 K (50 mW/cm^2, approximately 295–3000 nm, SOL2/500S, Honle UV Technology, Munchen, Germany) for 15 min in air at atmospheric humidity.

2.3. Characterization techniques

The morphology of pure cotton fibres and cotton fibres supported Ag–TiO_2 film were studied by scanning electron microscopy (Leica, Stereoscan 420) equipped with energy dispersive spectroscopic (EDS) microanalysis system (Oxford) and by means of atomic force microscopy AFM, on a Park Scientific Instrument Auto Probe LS.

Large-scale images are obtained in non-contact mode regime, using ultralevers Silicon conical tips with a typical radius of curvature of 100 Å (cantilever thickness = 2 μm; cantilever width = 28 μm; cantilever length = 85 μm; force constant = 17 N/m; nominal resonant frequency = 320 kHz). The AFM images were recorded in air at room temperature.

EDS analysis was also performed to verify the elemental composition of the deposited materials on the fibre surface. The UV–vis reflectance spectra were obtained at room temperature on a Perkin-Elmer UV–vis–NIR, to investigate the UV absorption properties, the location of the absorption edge and the quantum size effects [59] (if any) of the synthesized film.

XRD patterns have been collected by means of Philips PW1830 X-ray diffractometer in a Bragg Brentano configuration to identify the crystal phase and the structure. Co Kα radiation, 40 kV with 20 mA current, has been used. The obtained patterns have been analysed using Philips X'pert High score software and compared with standard patterns of International Center of Diffraction Data (ICDD) and powder Diffraction File (PDF) database.

Surface area has been obtained by N_2 adsorption at 77 K; with a commercial Micromeritics ASAP 2010 sorption analyzer.

Raman spectra were collected with a Renishaw in Via Raman Microscope Spectrometer equipped with Ar^+ laser beam emitting at 514 nm, at 8.2 mW output power. The photons scattered by the sample were dispersed by a 1800 lines/mm grating monochromator and simultaneously collected on a CCD camera, the collection optic was set at 50× objective.

To investigate the amount of Ag–TiO_2 deposited on the cotton fibres and the thermal stability of treated fibres, thermogravimetric analysis was performed in air flow (ramp 5 °C/min), by Universal 2050 TGA V5.4 A.

2.4. Photochromism experiment

The photochromism of the silver–titanium dioxide-coated cellulose fibres has been investigated by exposing alternatively the samples to ultraviolet and visible light irradiation. The ultraviolet light irradiation was performed for 15 min with a SOL2/500S lamp (50 mW/cm^2, Honle UV Technology, Munchen, Germany) simulating solar light and ranging from ultraviolet to infrared radiation (approximately 295–3000 nm). The irradiation with visible light was carried out using interior natural light. The photochromic effect caused by alternating exposure to ultraviolet and visible light were monitored by investigating the evolution of the UV–vis–NIR spectra of the system upon light exposure. For this purpose, *in situ* UV–vis reflectance experiments (in the 50,000–4000 cm^{-1} range and reported using the Kubelka–Munk function) were performed on the Ag–TiO_2-coated films. The colour changing cycles were repeated eight times on the same sample to check the photochromic behaviour and stability.

3. Results and discussion

3.1. SEM and EDS analyses

From SEM images, shown in Fig. 1, the surface morphology of the pure and sol–gel treated cotton fibres is compared. In particular Fig. 1(a) shows that the pure cotton fibres, although heterogeneous in nature, have average sizes in the 10–15 μm diameter range.

An enlarged view of a portion of a virgin fibre is shown in Fig. 1(b) where the presence of folds running along the elongation direction of the fibre is well evident. An enlarged view of a Ag–TiO_2 covered fibre is shown in Fig. 1(c). As the presence of Ag–TiO_2 coating clearly leads to partially filling of the folds characteristic of the virgin fibre, the formed coating appears homogeneously grafted on the fibre surface. The formation of firmly grafted films is likely associated with the high number of hydrophilic groups present on the cotton fibres, which are preferential anchoring sites for the deposition of TiO_2. The high ability of cotton fibres to support TiO_2 with respect to other supporting materials [60] is evident. At this level of magnification no evidence of silver particle could be shown. Further details of the morphology of fibres before and after Ag–TiO_2 coating will be shown by AFM measurements (*vide infra*). To quantify the amount of TiO_2 present on the fibres, one of the simplest method adopted was to burn the inorganic support and to weight the final inorganic residue. The resulting figure was in the 6–7 wt.% range (see below). However, the most interesting result, coming from this procedure, became evident from SEM analysis of the morphology of the inorganic residue.

In Fig. 2, the morphology of Ag–TiO_2 residue after burning at 500 °C for 5 h is reported. From this figure it is evident that the coating preserves the morphology of the original fibre. Due to the absence of the material inside after burning, the film structure is partially collapsed and damaged during the manipulation. From the film edges, the thickness of the layer can be inferred: the arrows indicate a thickness of ∼95–100 nm (inset of Fig. 2(a)

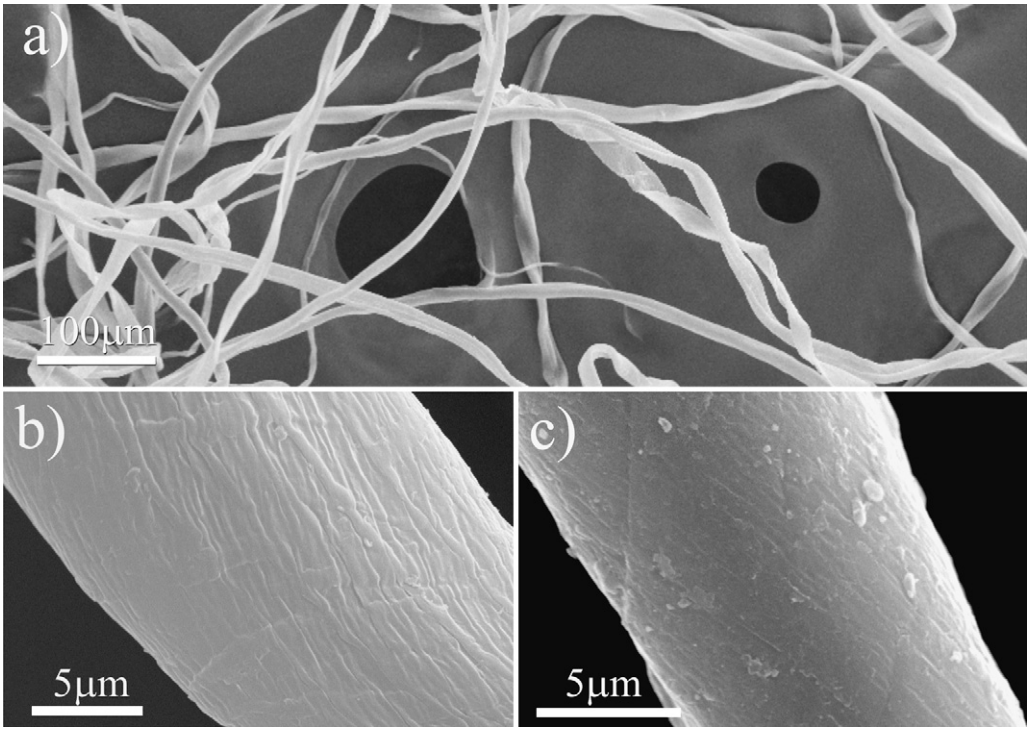

Fig. 1. (a) SEM image of a tangle of a pure cotton fibres; (b) SEM enlarged view of pure cotton fibre, shown in (a), where folds quite parallel to the fibre-axis are illustrated; (c) SEM enlarged view of a cotton fibre coated with a film of TiO_2 and silver nanoparticles.

and (b)). The BET results of the residual samples indicate that the film consists of porous materials of about 14 m^2/g surface area. From the SEM and AFM (*vide infra*) experiments no information about the state of the silver (particles or clusters) can be obtained. Conversely a suitable way to gain information on silver particles dispersed on the TiO_2 comes from EDS analysis. Fig. 3 represents the EDS quantitative analysis of the Ag–TiO_2 covered cotton fibre sample (part a) and of the Ag–TiO_2 film after combustion at 500 °C in air (part b). From these data, it comes out that on the Ag–TiO_2 covered cotton fibres (sample reported in Fig. 1(c)) the percentages of Ag and TiO_2 are 0.3 and 6 respectively. In particular it can be noticed that even if the content of Ag is very low, all the Ag peaks are almost detected and their intensities are enhanced after burning the organic core. Furthermore the C-peak disappears after the combustion treatment. It is worth noticing that the EDS results about TiO_2 concentration coincide with those obtained by weighting the residue after combustion.

3.2. Atomic force microscopy (AFM) analysis

Another approach to the investigation of the morphology of fibres is AFM. The obtained results on pure cotton fibre and on Ag–TiO_2-coated cotton fibre are imaged in Fig. 4(a) and (b). In particular, from Fig. 4(a) it is possible to notice that the pure fibre is characterized by structures parallel to the direction of the fibre axis. The surface average roughness is about 48.55 nm and the mean height about 123.1 nm (see Table 1). The values reported

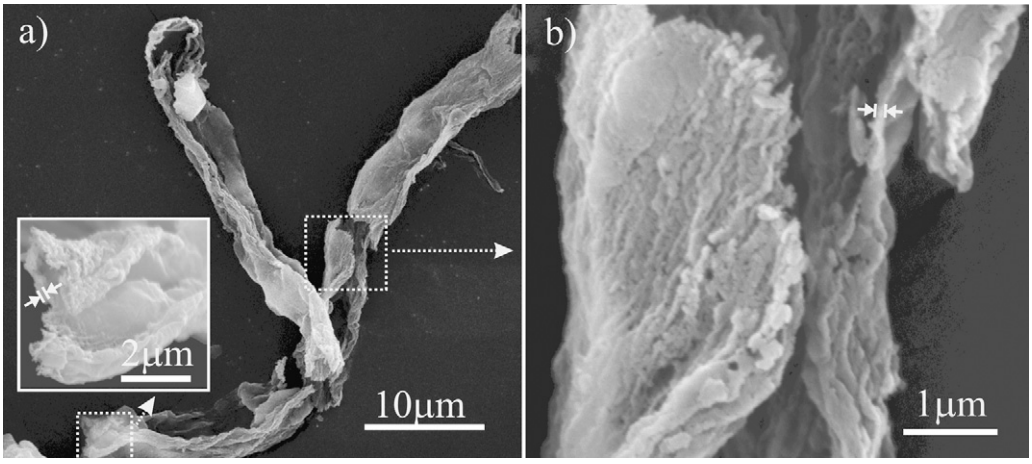

Fig. 2. (a) SEM image of cotton fibres covered with Ag–TiO_2 film burned at 500 °C for 5 h (b) enlarged view of a portion shown in (a).

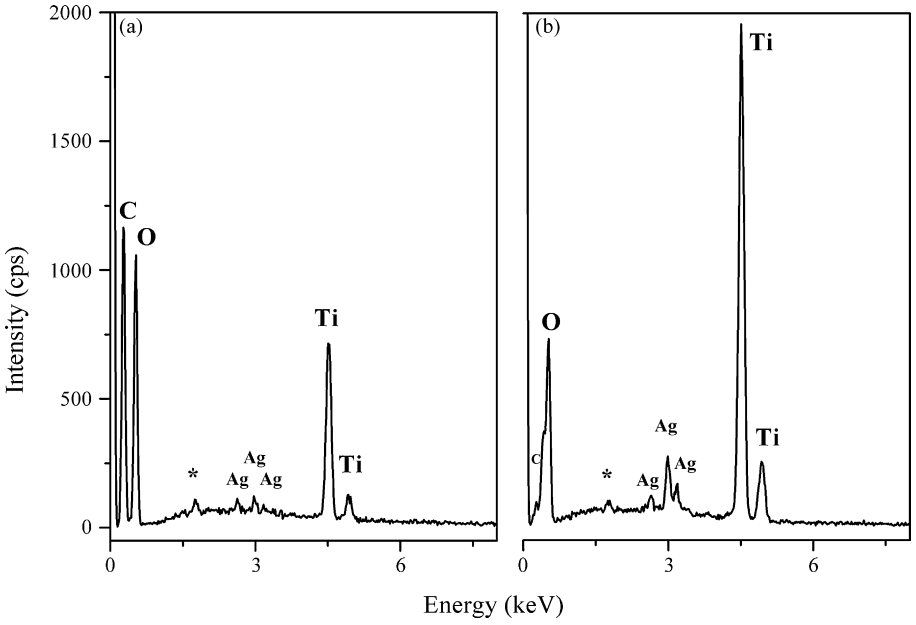

Fig. 3. EDS spectra of the Ag–TiO_2-coated cotton fibres before (a) and after combustion at 500 °C for 5 h (b) (* support).

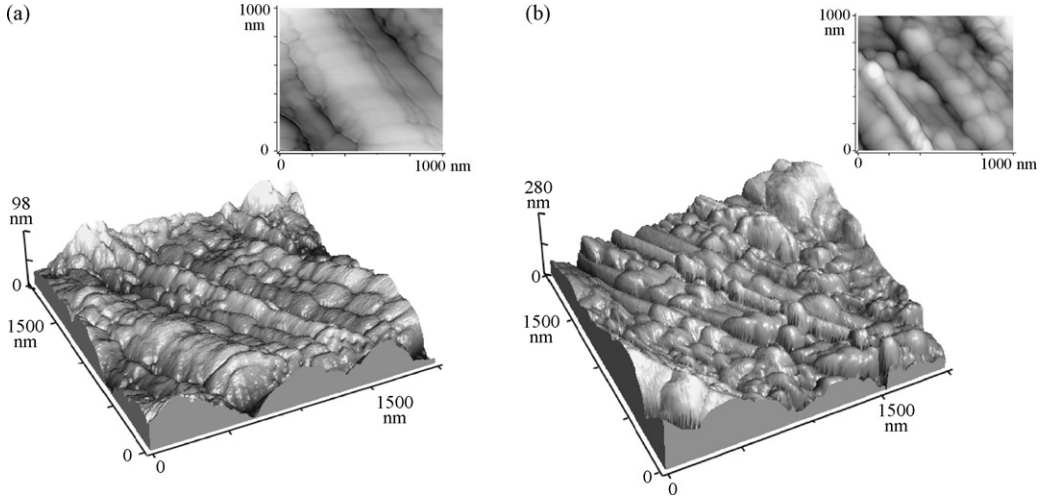

Fig. 4. (a) 3D *non-contact* AFM topographies of portion of a pure cotton fibre; (b) 3D *non-contact* AFM topographies of a Ag/TiO_2-coated cotton fibre. In the insets on top 3D enlarged views of portions of the fibres are shown.

in Table 1 were obtained from the region analysis within the selected areas, which allows to estimate the distribution of the heights (hystogram plots, not reported for sake of brevity). In the Ag–TiO_2-coated cotton fibre, the elongated structures are still visible. However new features are visible, which can be associated to TiO_2 particles aggregates, which are grafted to fibres.

The sample surface after coating with Ag–TiO_2 presents a mean height of about 481.0 nm and the average roughness is found to be of the order of 188.8 nm. The increased values of

Table 1
Region analysis values on selected area ((2x2) micron inside) of the three different samples

	Root-mean-squared roughness, R_{rms} (nm)	Average roughness, R_{ave} (nm)	Mean height	Median height
Pure fibre	54.67	48.55	123.1	129.4
Ag/TiO_2-coated fibre	228.0	188.8	481.0	469.7
Ag/TiO_2-coated fibre (burned)	209.2	178.1	403.8	360.9

$R_{rms} = \sqrt{\sum_{n=1}^{N}(z_n - \bar{z})^2/(N-1)}$, $R_{ave} = \sum_{n=1}^{N}|z_n - \bar{z}|/N$, where $\bar{z}$ = mean z height = $(1/N)\sum_{n=1}^{N} z_n$ and N is the number of data points within the height profile.

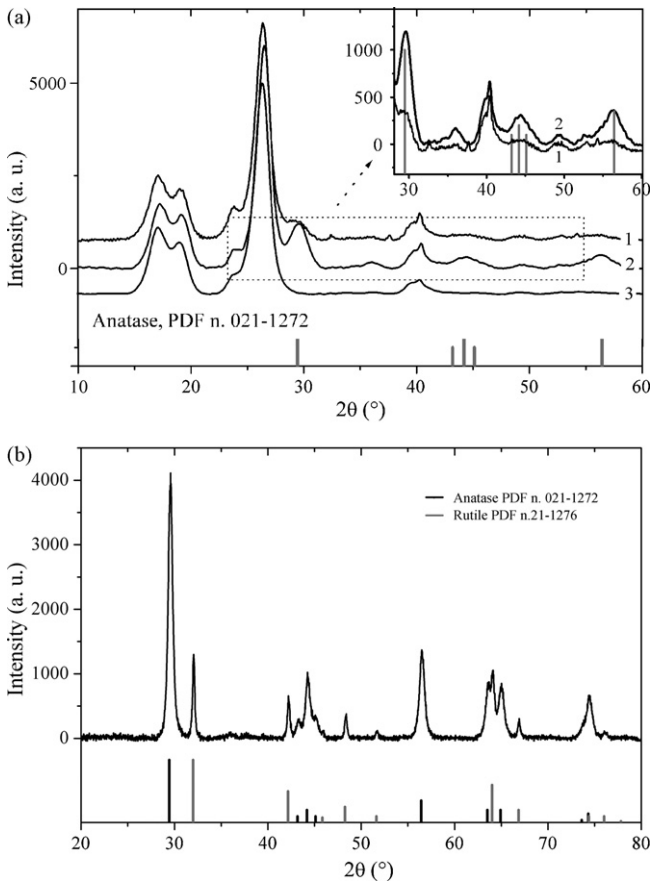

Fig. 5. (a) XRD pattern of Ag–TiO_2-coated (curve 1), TiO_2-coated (curve 2) and pure (curve 3) cotton fibres. The vertical lines, representing the peak positions of the standard anatase (PDF no. 021-1272), are reported below the XRD pattern. The most intense XRD diffraction peaks are related to cellulose. In the inset, the most representative portion of the pattern, showing the TiO_2 anatase phases, is reported. (b) XRD pattern of Ag–TiO_2 film. The vertical black lines indicate anatase and grey lines rutile TiO_2 phases (related SEM images are reported in Fig. 2. For detail see the text).

heights and roughness, as compared to the pure fibre, can be explained with the presence of TiO_2 thin layer on the elongated structures of the fibre. From AFM images too, at this level of magnification, it is not possible to evidence the presence of both single TiO_2 and of single Ag particles, because of low-resolution conditions.

3.3. X-ray diffraction (XRD) analysis

The XRD patterns of the pure, TiO_2 and of Ag–TiO_2-coated cotton fibres are illustrated in Fig. 5(a). In the inset, an exploded view shows the patterns of the TiO_2 and Ag–TiO_2 impregnated sample together with the position of the peaks of anatase taken from the reference. Two of three major peaks at 17.16° and 19.12°, are related to amorphous phase of cotton fibre, while the peak at 26.4° is due to the crystalline phase [61]. The three broader peaks at 29.44°, 44.192° and 56.40° are indicative of anatase phase. The remarkable width of these peaks suggests that the particles sizes of the deposited photocatalyst are quite small. From the full width at half maximum (FWHM) of the peaks at 29.44° and 56.40° by using Scherrer's equation, $L_c = K\lambda/(\beta \cos\theta)$ [62] (where λ is the X-ray wavelength, β the FWHM of the diffraction line, θ the diffraction angle, and K is a constant, which has been assumed to be 0.9), an average particles diameter of silver-doped TiO_2 is estimated to be about 3.5 nm, while that of the TiO_2 particles on the TiO_2 film is about 5.0 nm.

From this, it is evident that the silver doping reduces the particle size of TiO_2, a fact which could be favourable to photocatalytic efficiency. We will see in the following that the XRD results are in strong agreement with the UV–vis and Raman results (*vide infra*). The silver nanoparticles supported on the TiO_2 phase are not detectable. XRD patterns were collected also on the sample obtained after combustion overnight at 500 °C (hollow cylindrical shaped material described before). From Fig. 5(b) it results that at about 500 °C the entire fibre covered by the Ag–TiO_2 film is destroyed and within the film materials only a little amount of the anatase TiO_2 is converted to rutile phase. This means that the deposited nanosized TiO_2 anatase phase remains substantially unchanged even at high temperature. The peak related to cellulose phase, which is dominating the Ag–TiO_2-coated cellulose pattern (Fig. 5(a)), is now completely disappeared.

3.4. Raman spectra

Raman analysis represents a valuable information about the properties of the cotton fibres supported Ag–TiO_2 film (Fig. 6). From Raman spectra reported in Fig. 6, curve 1 represents Ag–TiO_2 covered cotton fibres, while curve 2 reports the TiO_2 covered cotton fibres. For comparison, the Raman spectra of the cotton fibre (curve 3) and pure anatase TiO_2 (curve 4) are reported. It can be immediately seen that the spectrum of the Ag–TiO_2 and TiO_2-coated cotton fibres (curves 1 and 2, respectively) is dominated by peaks at 157, 406, 517 and 639 cm^{-1}, presumably associated with TiO_2 phase. This assignment can

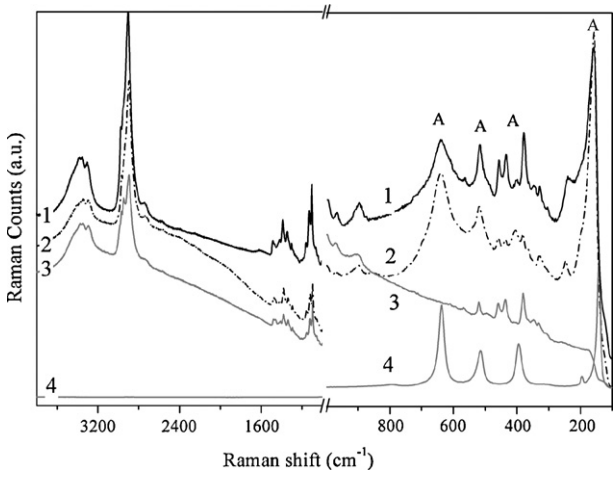

Fig. 6. Raman spectra of the Ag–TiO_2-coated (1, black solid line), TiO_2-coated (2, dot dashed line) and pure cotton fibres (3, grey solid line). For comparison, the Raman spectrum of pure anatase TiO_2 is reported (4, grey solid line). Notice that in the 3750–900 cm^{-1} range all bands of curves 1–and 3 are related to the cotton fibres (cellulose), whereas in the 800–190 cm^{-1} range Raman features of anatase TiO_2 and of the fibres are both present (A indicates anatase phase TiO_2).

be confirmed by comparison with the Raman spectrum of pure anatase TiO_2 (curve 4), which shows bands at 143, 396, 515, and 637 cm^{-1}. Of course, pure cotton fibres, treated with blank sol, show no peaks regarding TiO_2 (curve 3). It can be argued that Raman technique is useful to reveal the presence of TiO_2 particles on the external surface of the film. Furthermore it can be noticed that the Raman peaks of the supported TiO_2 are much broader than those of the pure anatase: an explanation of the increase of the peak half width can be advanced. For instance, Raman studies of nanosized anatase phase TiO_2, produced by sol gel route at low temperatures (i.e. lower than 100 °C), report that the vibrational features of TiO_2 are slightly dependent upon the particles sizes and crystallinity [1].

In particular, smaller and less crystalline particles are characterized by broader Raman peaks. The silver-doped TiO_2 samples are constituted by particles with diameter lower than 3.5 nm. Another interesting observation concerns the position of Raman band at 160 cm^{-1}, which is distinctly upward shifted with respect to that of pure anatase (143 cm^{-1}). Choi et al. [63] have suggested that the Raman bands shift towards higher frequency values as the particles sizes decrease. In particular, when the particles sizes decrease to the nanometer scale, the lowest Raman band shifts towards higher frequency values, due to the increasing force constants [64,65]. As a similar shift is observed on our sample, we can conclude that Raman spectroscopy reveals information on the presence of a TiO_2 nanostructured layer, which can be constituted by particles with diameter $\leq$3.5 nm.

3.5. Thermal analysis (TGA and DTGA)

Fig. 7 reports the TGA (grey line) and DTGA (black line) analyses, carried out in air, under heat flow response, of Ag–TiO_2-coated fibres. The TGA results of the sample show two major exothermic peaks and a weight decrease (~2.5%), which can be associated with H_2O desorption. After combustion of the organic part, a residue of ~6.2% by weight is still present on the fibres. From these results and from the SEM and EDS analyses (before described), it is confirmed the presence of a photocatalytically efficient Ag–TiO_2 layer on the fibres surface.

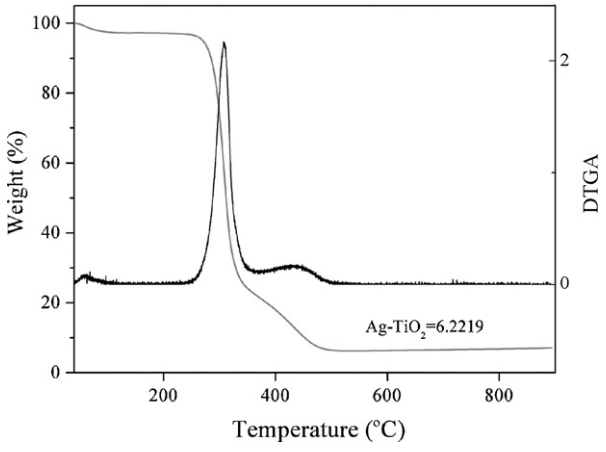

Fig. 7. Thermal degradation of Ag–TiO_2 covered cotton fibres under air flow; TGA (grey line) and DTGA (black line) curves of the Ag–TiO_2-coated cotton fibres (ramp 5 °C/min, in air, 40–900 °C) are shown. A residual weight of about 6% has been obtained at 900 °C. This value is due to the Ag–TiO_2 contents in the sample.

3.6. UV–vis reflectance spectra and photochromic effect

Fig. 8(a) shows the UV–vis reflectance spectra of the pure cotton fibre (curve 1), cotton fibres covered with TiO_2 (curve 3), Ag–TiO_2-coated cotton fibres exposed to visible (curve 4) and to ultraviolet light for 15 min (curve 5). Also the reflectance of pure anatase TiO_2 is shown as reference (curve 2). TiO_2 (curve

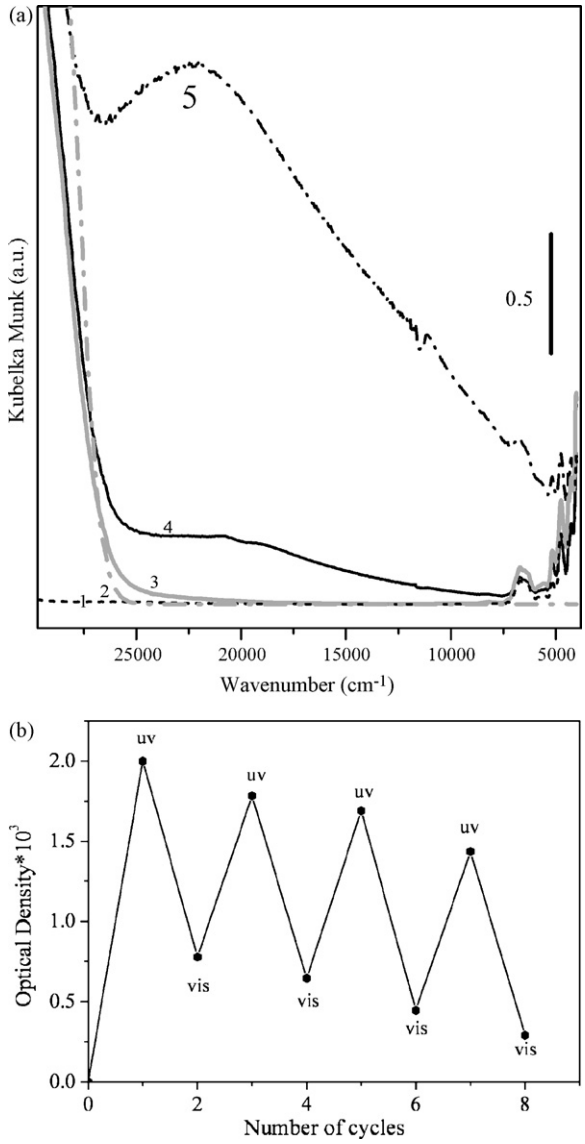

Fig. 8. (a) UV–vis reflectance spectra of fibres treated with blank sol (1, dash black line), anatase TiO_2 (2, grey dash dot line), TiO_2-coated cotton fibres (3, solid grey line), Ag–TiO_2-coated cotton fibres under visible light exposure (4, black solid line) and Ag–TiO_2-coated cotton fibres under 15 min UV light exposure (5, dash dot black line). This absorption band is related to the different optical properties of the Ag–TiO_2 coating under alternative ultraviolet/visible light exposures. (b) Optical density of the absorption band between 26,750 and 7000 cm^{-1}. The sequence of the light exposure cycles represents the alternative and reversible optical behaviour after ultraviolet (maxima) and visible (minima) light irradiations.

2), TiO_2 covered fibres (curve 3) and TiO_2–Ag film (curve 4) all show an absorption edge at above 29,000 cm^{-1} associated with the optical gap typical of the anatase phase. With regards to pure cotton fibres (curve 1) no absorption edge is present. The absorption edge at ~29,000 cm^{-1}, observed for TiO_2 and Ag–TiO_2-coated cotton fibres (curves 3 and 4), is very similar to that of pure anatase TiO_2 (curve 2): the presence of TiO_2 anatase phase on the cotton fibres is then confirmed. The slightly upward shifted absorption edge suggests that the particles sizes of the photocatalyst are smaller than those of anatase (quantum size effect). This observation is in agreement with the result obtained from XRD pattern. Coming now to curve 4, the presence of a complex absorption centered at ~22.000 cm^{-1} is strongly indicating the presence of Ag particles on the TiO_2 film (since Ag^+ does not have absorption in this range). The changes of colour upon exposure to light is well known. Upon exposure to UV light, the intensity of the ~22,000 cm^{-1} absorption (showing a tail extending in the NIR) is strongly enhanced. This is due to the reduction of Ag^+ to Ag° and formation of $(Ag^\circ)_n$ clusters. The colour of the sample changes from light grey to brown.

It is well known that the resonance wavelength is blue shifted as the dimensions of Ag nanoparticles are decreasing [50,56]. On this basis, the broad absorption centered at ~22,000 cm^{-1} is associated to a broad distribution of Ag particles. As a matter of fact, a different colour for the Ag–TiO_2-coated fibre, upon exposure to light with different wavelengths, have been observed [55]. Furthermore, it is known that Ag particles deposited on TiO_2 are responsible for multi colour photochromic behaviour. This is explained with the anisotropic character of Ag nanoparticles, which have two different resonance wavelengths in the porous TiO_2 film [57]. It is known that, after photon absorption, the presence of silver nanoparticles promotes the charge separation of the electron–hole pairs from TiO_2, by acting as an electron sink [54]. Also the plasmon resonance in metallic Ag nanoparticles is considered to locally enhance the electric field, facilitating electron–hole production [66]. It has been pointed out that due to addition of Ag nanoparticles to TiO_2 film, smaller TiO_2 grain sizes can be found. An explanation of this result is difficult. Kato et al. [67] explained that photodeposition of Ag on a TiO_2 film enhanced photocatalytic degradation of gaseous sulphur compounds and suggested that Ag acted as a co-catalyst. However an hypothesis was advanced about the Ag-TiO_2 interaction. Moreover, Brook et al. [54] believe that there is no chemical interaction between the Ag and the TiO_2, although the Ag and TiO_2 layers were grown sequentially. However the problem concerning the effect of silver doping on decreasing the size of TiO_2 particles cannot be solved on the basis of our results. In Fig. 8(b), a sequence of light exposure cycles to visible and ultraviolet irradiation is shown. This sequence causes the fibres to become alternatively brown under ultraviolet light and white grey under visible light and this behaviour can be repeated several times without substantial modification. We so conclude that Ag-TiO_2 cotton fibres show alternative photochromic effects. Work is in progress to estimate whether Ag-TiO_2 particles can display photo enhanced self-cleaning and bioactivity.

4. Conclusion

We have developed a new and simple process to deposit silver nanoparticles doped TiO_2 for photochromic application. The morphological studies and the characterization results indicate that the deposition of Ag–TiO_2 coating on the cotton fibres and the curing at low temperature, have not changed the basic chemical and physical properties of the cotton fibres. In addition, we can conclude that the Ag–TiO_2 thin film will act as a photoactive materials of multi functionality. Furthermore we expect that the film display biocidal functionality to bacteria, phtochtomism (Ag particles) and photoactivity for self-cleaning (TiO_2 phase).

Acknowledgements

The authors acknowledge the financial support from Regione Piemonte (Progetto NANOMAT, Docup 2000-2006, Linea 2.4a).M.Jasim Uddin is grateful to AssociazioneTessile e Salute for supporting his PhD fellowship.

References

[1] (a) A. Fujishima, K. Honda, Nature 238 (1972) 37–38;
(b) D. Bersani, G. Antonioli, P.P. Lottici, T. Lopez, J. Non-Cryst. Solids 234 (1998) 175–181.
[2] A. Matsuda, Y. Kotani, T. Kogure, M. Tatsumisago, T. Minami, J. Am. Ceram. Soc. 83 (2000) 229–231.
[3] Y. Djaoued, S. Badilescu, P.V. Ashrit, D. Bersani, P.P. Lottici, R. Bruning, J. Sol–Gel Sci. Technol. 24 (2002) 247–254.
[4] H. Yamashita, M. Harada, A. Tanii, M. Honda, M. Takeuchi, Y. Ichihashi, M. Anpo, N. Iwamoto, N. Itoh, T. Hirao, Catal. Today 63 (2000) 63–69.
[5] M. Keshmiri, M. Mohseni, T. Troczynski, Appl. Catal. B: Environ. 53 (2004) 209–219.
[6] M.J. Uddin, F. Cesano, F. Bonino, S. Bordiga, G. Spoto, D. Scarano, A. Zecchina, J. Photochem. Photobiol. A: Chem. 89 (2007) 286–294.
[7] R. Isono, T. Yoshimura, K. Esumi, J. Colloid Interface Sci. 288 (2005) 177–183.
[8] D. Chatterjee, S. Dasgupta, J. Photochem. Photobiol. C 6 (2005) 186–205.
[9] M. Anpo, M. Takeuchi, J. Catal. 216 (2003) 505–516.
[10] O. Carp, C.L. Huisman, A. Reller, Prog. Solid State Chem. 32 (2004) 33–177.
[11] W.Y. Choi, A. Termin, M.R. Hoffmann, J. Phys. Chem. 98 (1994) 13669–13679.
[12] C.-G. Wu, C.-C. Chao, F.-T. Kuo, Catal. Today 97 (2004) 103–112.
[13] S. Rodrigues, K.T. Ranjit, S. Uma, I.N. Martyanov, K.J. Klabunde, J. Adv. Mater. 17 (2005) 2467–2471.
[14] P.N. Kapoor, S. Uma, S. Rodriguez, K.J. Klabunde, J. Mol. Catal. A 229 (2005) 145–150.
[15] S. Yin, Q.W. Zhang, F. Saito, T. Sato, Chem. Lett. 32 (2003) 358–359.
[16] R. Asahi, T. Morikawa, T. Ohwaki, K. Aoki, Y. Taga, Science 293 (2001) 269–271.
[17] I.N. Martyanov, S. Uma, S. Rodrigues, K. Klabunde, J. Chem. Commun. (2004) 2476–2477.
[18] C. Di Valentin, G. Pacchioni, A. Selloni, S. Livraghi, E. Giamello, J. Phys. Chem. B 109 (2005) 11414–11419.
[19] S. Livraghi, A. Votta, M.C. Paganini, E. Giamello, Chem. Commun. (2005) 498–500.
[20] S. Livraghi, M.C. Paganini, E. Giamello, A. Selloni, C. Di Valentin, G. Pacchioni, J. Am. Chem. Soc. 128 (2006) 15666–15671.
[21] A. Ghicov, J.M. Macak, H. Tsuchiya, J. Kunze, V. Haeublein, L. Frey, P. Schmuki, Nano Lett. 6 (2006) 1080–1082.
[22] M. Batzill, E.H. Morales, U. Diebold, Phys. Rev. Lett. (2006) 96.

[23] T. Yamaki, T. Umebayashi, T. Sumita, S. Yamamoto, M. Maekawa, A. Kawasuso, H. Itoh, Nucl. Instrum. Methods Phys. Res., Sect. B 206 (2003) 254–258.
[24] Y. Choi, T. Umebayashi, S. Yamamoto, S. Tanaka, J. Mater. Sci. Lett. 22 (2003) 1209–1211.
[25] S. Sakthivel, H. Kisch, Angew. Chem., Int. Ed. 42 (2003) 4908–4911.
[26] X.T. Hong, Z.P. Wang, W.M. Cai, F. Lu, J. Zhang, Y.Z. Yang, N. Ma, Y. Liu, J. Chem. Mater. 17 (2005) 1548–1552.
[27] S. Usseglio, A. Damin, D. Scarano, S. Bordiga, A. Zecchina, C. Lamberti, J. Am. Chem. Soc. 129 (2007) 2822–2828.
[28] H.M. Luo, T. Takata, Y.G. Lee, J.F. Zhao, K. Domen, Y. Yan, Chem. Mater. 16 (2004) 846–849.
[29] T. Lana-Villarreal, A. Rodes, J.M. Perez, R. Gomez, J. Am. Chem. Soc. 127 (2005) 12601–12611.
[30] K. Kalyanasundaram, M. Gratzel, N. Vlachopoulos, V. Krishnan, A. Monnier, J. Phys. Chem. 91 (1987) 2342–2347.
[31] F.R.F. Fan, A.J. Bard, J. Am. Chem. Soc. 101 (1979) 6139–6140.
[32] F. Xamena, P. Calza, C. Lamberti, C. Prestipino, A. Damin, S. Bordiga, E. Pelizzetti, A. Zecchina, J. Am. Chem. Soc. 125 (2003) 2264–2271.
[33] P. Calza, C. Paze, E. Pelizzetti, A. Zecchina, Chem. Commun. (2001) 2130–2131.
[34] R.F. Howe, Y.K. Krisnandi, Chem. Commun. (2001) 1588–1589.
[35] P.D. Southon, R.F. Howe, Chem. Mater. 14 (2002) 4209–4218.
[36] V. Luca, M. Osborne, D. Sizgek, C. Griffith, P.Z. Araujo, Chem. Mater. 18 (2006) 6132–6138.
[37] S. Usseglio, P. Calza, A. Damin, C. Minero, S. Bordiga, C. Lamberti, E. Pelizzetti, A. Zecchina, Chem. Mater. 18 (2006) 3412–3424.
[38] Y.K. Krisnandi, E.E. Lachowski, R.F. Howe, Chem. Mater. 18 (2006) 928–933.
[39] E. Borello, C. Lamberti, S. Bordiga, A. Zecchina, C. Otero Arean, Appl. Phys. Lett. 71 (1997) 2319–2321.
[40] C. Lamberti, Micropor. Mesopor. Mater. 30 (1999) 155–163.
[41] S. Bordiga, G.T. Palomino, A. Zecchina, G. Ranghino, E. Giamello, C. Lamberti, J. Chem. Phys. 112 (2000) 3859–3867.
[42] A. Damin, F.X.L. Xamena, C. Lamberti, B. Civalleri, C.M. Zicovich-Wilson, A. Zecchina, J. Phys. Chem. B 108 (2004) 1328–1336.
[43] C. Prestipino, P.L. Solari, C. Larnberti, J. Phys. Chem. B 109 (2005) 13132–13137.
[44] S. Uma, S. Rodrigues, I.N. Martyanov, K.J. Klabunde, Micropor. Mesopor. Mater. 67 (2004) 181–187.
[45] A.D. Russell, W.B. Hugo, Antimicrobial activity and action of silver, in: G.P. Ellis, D.K. Luscombe (Eds.), Progress in Medicinal Chemistry, vol. 31, Elsevier Science, St. Louis, MO, 1994, p. 351.
[46] S. Silver, FEMS Microbiol. Rev. 27 (2003) 341.
[47] E. Verne, S. Di Nunzio, M. Bosetti, P. Appendino, C.V. Brovarone, G. Maina, M. Cannas, Biomaterials 26 (2005) 5111–5119.
[48] S. Thomas, P. McCubbin, J. Wound Care 12 (2003) 101.
[49] K. Dunn, V. Edwards-Jones, Burns 30 (2004) S1.
[50] J.J. Mock, M. Barbic, D.R. Smith, D.A. Schultz, S. Schultz, J. Chem. Phys. 116 (2002) 6755–6759.
[51] F.R.F. Fan, A.J. Bard, J. Phys. Chem. B 106 (2002) 279–287.
[52] T. Yuranova, A.G. Rincon, A. Bozzi, S. Parra, C. Pulgarin, P. Albers, J. Kiwi, J. Photochem. Photobiol. A: Chem. 161 (2003) 27–34.
[53] Q.L. Feng, J. Wu, G.Q. Chen, F.Z. Cui, T.N. Kim, J.O. Kim, J. Biomed. Mater. Res. 52 (2000) 662–668.
[54] L.A. Brook, P. Evans, H.A. Foster, M.E. Pemble, A. Steele, D.W. Sheel, H.M. Yates, J. Photochem. Photobiol. A: Chem. 187 (2007) 53–63.
[55] Y. Ohko, T. Tatsuma, T. Fujii, K. Naoi, C. Niwa, Y. Kubota, A. Fujishima, Nat. Mater. 2 (2003) 29–31.
[56] R.C. Jin, Y.W. Cao, C.A. Mirkin, K.L. Kelly, G.C. Schatz, J.G. Zheng, Science 294 (2001) 1901–1903.
[57] K. Naoi, Y. Ohko, T. Tatsuma, J. Am. Chem. Soc. 126 (2004) 3664–3668.
[58] B. Ohtani, Y. Okugawa, S. Nishimoto, T. Kagiya, J. Phys. Chem. 91 (13) (1987) 3550–3555.
[59] P.F. Fu, Y. Luan, X.G. Dai, J. Mol. Catal. A: Chem. 221 (2004) 81–88.
[60] Y.C. Dong, L.W. Zhang, R.H. Liu, T. Zhu, J. Appl. Polym. Sci. 99 (2006) 286–291.
[61] M.A. Moharram, T.Z.A.E. Nasr, N.A. Hakeem, J. Pol. Sci.: Pol. Lett. Ed. 19 (1981) 183–187.
[62] L.S. Birks, H. Friedman, J. Appl. Phys. 17 (1946) 687–692.
[63] H.C. Choi, Y.M. Jung, S.B. Kim, Vib. Spectrosc. 37 (2005) 33–38.
[64] J. Rockenberger, L. Troger, A. Kornowski, T. Vossmeyer, A. Eychmuller, J. Feldhaus, H. Weller, J. Phys. Chem. B 101 (1997) 2691–2701.
[65] M.A. Marcus, M.P. Andrews, J. Zegenhagen, A.S. Bommannavar, P. Montano, Phys. Rev. B 42 (1990) 3312–3316.
[66] J.M. Herrmann, H. Tahiri, Y. AitIchou, G. Lassaletta, A.R. GonzalezElipe, A. Fernandez, Appl. Catal. B: Environ. 13 (1997) 219–228.
[67] S. Kato, Y. Hirano, M. Iwata, T. Sano, K. Takeuchi, S. Matsuzawa, Appl. Catal. B: Environ. 57 (2005) 109–115.